

L-Verse: Bidirectional Generation Between Image and Text

Taehoon Kim* Gwangmo Song Sihaeng Lee Sangyun Kim Yewon Seo
 Soonyoung Lee Seung Hwan Kim Honglak Lee Kyunghoon Bae
 LG AI Research

Abstract

Far beyond learning long-range interactions of natural language, transformers are becoming the de-facto standard for many vision tasks with their power and scalability. Especially with cross-modal tasks between image and text, vector quantized variational autoencoders (VQ-VAEs) are widely used to make a raw RGB image into a sequence of feature vectors. To better leverage the correlation between image and text, we propose L-Verse, a novel architecture consisting of feature-augmented variational autoencoder (AugVAE) and bidirectional auto-regressive transformer (BiART) for text-to-image and image-to-text generation. Our AugVAE shows the state-of-the-art reconstruction performance on ImageNet1K validation set, along with the robustness to unseen images in the wild. Unlike other models, BiART can distinguish between image (or text) as a conditional reference and a generation target. L-Verse can be directly used for image-to-text or text-to-image generation tasks without any finetuning or extra object detection frameworks. In quantitative and qualitative experiments, L-Verse shows impressive results against previous methods in both image-to-text and text-to-image generation on MS-COCO Captions. We furthermore assess the scalability of L-Verse architecture on Conceptual Captions and present the initial results of bidirectional vision-language representation learning on general domain.

1. Introduction

Text-to-image generation and image captioning can be summarized as a task of learning cross-modal representations of image and text. Recent studies [7, 10, 11, 31] on vision-language tasks have highly improved the performance of each target task, in particular with various transformer architectures [3, 4, 9, 42]. Initially designed to understand natural language, the *dot-product multi-head attention mechanism* [42] effectively learns long-range interactions of sequential data. To leverage transformer archi-

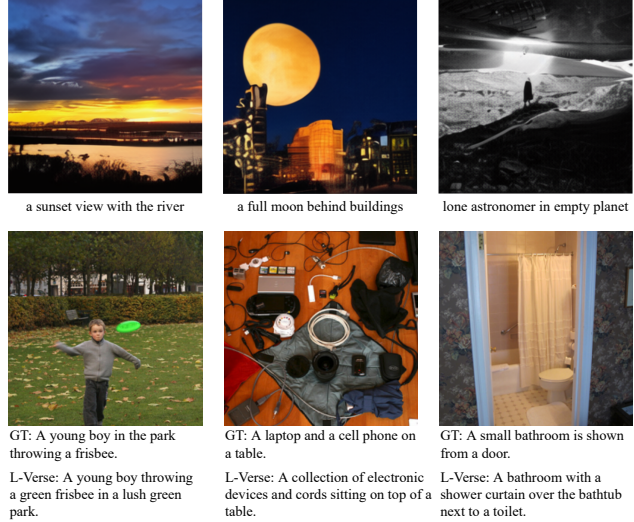


Figure 1. Examples of L-Verse on zero-shot text-to-image generation on Conceptual Captions (top) and image-to-text generation on MS-COCO Captions (bottom). Trained in bidirectional manner, L-verse can both generate well-conditioned synthetic images and detailed captions without any finetuning.

tures [42] also in vision domains, the input image are factorized into a sequence of latent feature vectors.

To encode an image into a sequence of latent feature vectors, the vector quantized variational autoencoder (VQ-VAE) [41] can be used to learn a discrete latent representation with quantized embedding vectors from the *visual codebook*. VQ-VAE is a simple and powerful representation learning method to make image sequential and is widely used in conditional image generation tasks with auto-regressive pairs like RNNs [32, 41] or transformers [10–12, 31]. Improving the reconstruction quality of VQ-VAE is also an active area of research [12, 31, 32].

Combining an auto-regressive transformer [3] with feature extractor like VQ-VAEs or other deep convolutional neural networks (CNNs) is becoming a popular approach for various vision-language tasks. However, training a model for unidirectional text-to-image [10, 31] or image-to-text [7] generation task still requires a large amount of

*Correspondence to: taehoon.kim@lgresearch.ai

data or an extra object detection framework. We hypothesize that learning bidirectional cross-modal representation of image and text can alleviate this problem via better data efficiency.

This paper proposes an approach, *L-Verse* (*latent verse*), for learning a bidirectional vision-language cross-modal representation. The key idea of L-Verse is two-fold: (*i*) augment a visual codebook with diverse features and (*ii*) enable an auto-regressive transformer to learn bidirectional image-text generation. Our novel *cross-level feature augmentation technique* effectively increase the diversity of a visual codebook with unique feature embedding vectors. We furthermore add a *segment embedding* to an auto-regressive transformer [3] to teach the difference between image (or text) as given condition or generation target. Specifically, our contribution for vision-language cross-modal representation learning are summarized as follows:

- We introduce a feature-augmented variational autoencoder (AugVAE), a VQ-VAE trained with cross-level feature augmentation. With the feature-augmented visual codebook, AugVAE shows the state-of-the-art reconstruction performance on both in-domain ImageNet1K [8] validation set (Figure 2) and out-of-domain image datasets (Figure 5).
- We propose a bidirectional auto-regressive transformer (BiART) for bidirectional image-text generation. We index each token with two different embedding vectors according to its role as a conditional reference ([REF]) or a generation target ([GEN]). With this segment embedding, our BiART can both generate corresponding images to given texts or meaningful captions to given images without any finetuning.
- Trained with AugVAE and BiART, L-Verse outperforms previously proposed image captioning models in most of machine evaluation metrics on MS-COCO Captions [24] *Karpathy* test split. It is also notable that L-Verse does not require any object-detection frameworks, such as Faster-RCNN [33].
- L-Verse shows comparable text-to-image generation results to other generative models on MS-COCO Captions [24]. We also assess the scalability of L-Verse for zero-shot text-to-image generation by training on Conceptual Captions [37].

Section 2 briefly reviews previous works on VQ-VAE and cross-modal vision-language tasks. Section 3 explains how we design AugVAE and BiART to learn the *bidirectional* cross-modal representation between image and text. Section 4 shows quantitative and qualitative results on image reconstruction, image captioning, and text-to-image generation. Section 5 summarizes our paper with conclusion and discussion for future works.

2. Related Work

Adapting transformer architectures [3, 4, 9, 42] for various vision-language tasks has been an active research area in the recent years. Since an image is a matrix of RGB pixel values, it should be first factorized into a sequence of feature vectors. Recent auto-regressive transformer based generative models [10, 12, 31] utilize different variants of VQ-VAE [41] to compress and reconstruct images. In this section, we introduce the main concept of VQ-VAE and its variants. We also explain how VQ-VAE or other CNN architectures are combined with auto-regressive transformers to solve text-to-image or image-to-text generation tasks.

2.1. Vector Quantized Variational Autoencoder

Vector quantized variational autoencoder, VQ-VAE [41], is a set of an encoder E , a decoder D , and a visual codebook Z for learning discrete representations of images. The CNN encoder E factorizes the continuous representation of an image \hat{z} into series of discrete vectors z_q , each selected from visual codebook Z . The CNN decoder D is used to reconstruct any z_q sampled from Z . Razavi *et al.* [32] extend this approach to use hierarchical feature representation and apply exponential-moving-average (EMA) weight update to codebook Z . To better optimize the training of VQ-VAE, Ramesh *et al.* [31] use the gumbel-softmax relaxation [18, 27]. Esser *et al.* [12] further improve the quality of image reconstruction with additional CNN discriminator, originated from generative adversarial network (GAN) [13].

2.2. Text-to-Image Generation

Generative adversarial networks (GANs) [40, 45, 48, 50] have been traditionally used for text-conditional image generation tasks. GAN based models focus on finding better modeling assumptions for specific data domains like CUB-200 [44] or MS-COCO Captions [24]. Ramesh *et al.* [31] first trained a 12-billion parameter transformer [4] on 250-million image-text pairs for text-to-image generation in the general domain. Ding *et al.* [10] proposed a 4-billion parameter transformer, CogView, with stable training techniques and finetuning strategies for various downstream tasks.

2.3. Image-to-Text Generation

As the *dot-product multi-head attention* [42] was initially designed for language tasks, transformers have achieved new state-of-the-art results in generating natural and detailed captions corresponding to an input image. M^2 Transformer [7] utilized region features extracted using Faster R-CNN [33] to generate captions for each image. While visual semantics of each region improves the quality, objects outside detection target classes (80 classes for MS-COCO Detection [24]) get ignored.

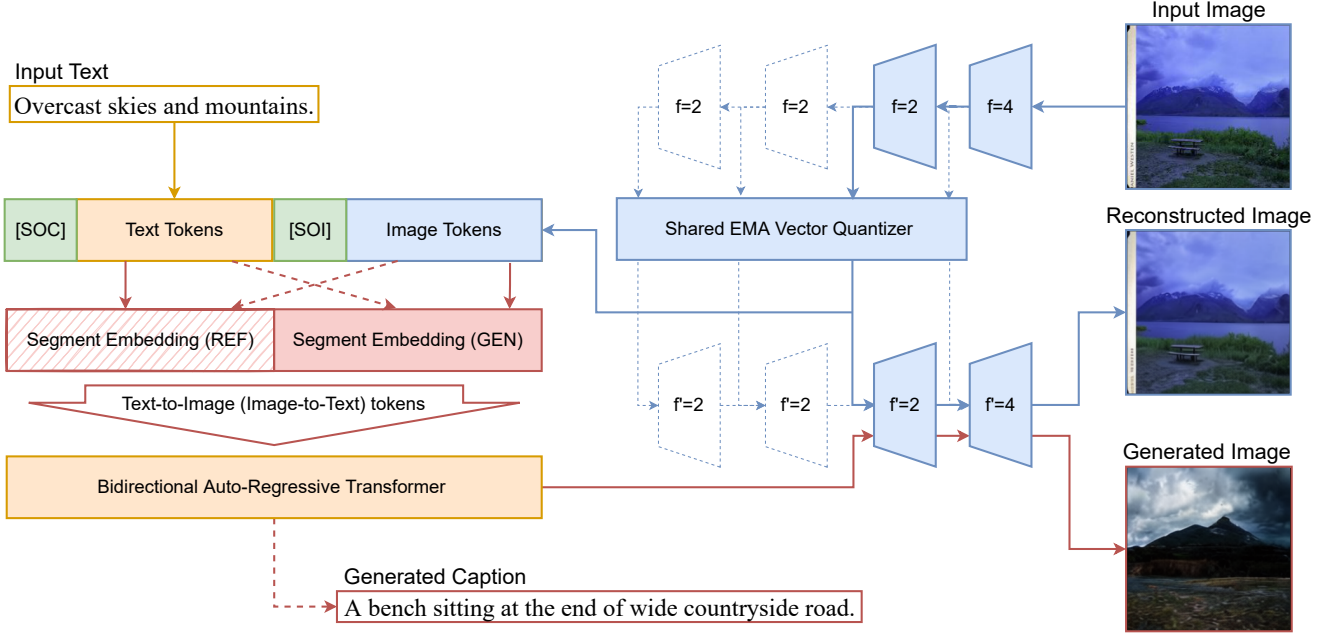


Figure 2. Proposed L-Verse framework. [SOC] : Start of Caption (text) token. [SOI] : Start of Image token. Feature-augmented variational autoencoder (AugVAE) in *blue*. Bidirectional auto-regressive transformer (BiART) in *red*. AugVAE encoder E encodes an image x into tokens z . Segment embedding indicates each token as a conditional reference (REF), or a generation target (GEN). BiART T either can generate image tokens $T(y)$ from input text y or caption $G(z)$ from z . AugVAE decoder G decodes z and $T(y)$ into RGB images.

3. Method

3.1. Preliminary

Ramesh *et al.* [31] proposed a two-stage training procedure for text-to-image generation with an auto-regressive transformer [3] :

- **Stage 1:** Train a discrete variational autoencoder (dVAE) [31] to compress each 256×256 RGB into a 32×32 grid of image tokens with each element of 8192 (d_Z) possible values .
- **Stage 2:** Concatenate up to 256 BPE-encoded text tokens with the $32 \times 32 = 1024$ image tokens, and train an auto-regressive transformer [3] to model the joint distribution over text and image tokens.

The approach maximizes the evidence lower bound [20, 35] on the joint likelihood of the model distribution over the image x , the caption y , and the tokens z for the encoded RGB image. From the factorization $p_{\theta, \psi}(x, y, z) = p_{\theta}(x|y, z)p_{\psi}(y, z)$, the lower bound is yielded as

$$\ln p_{\theta, \psi}(x, y) \geq \mathbb{E}_{z \sim q_{\phi}(z|x)} (\ln p_{\theta}(x|y, z) - D_{KL}(q_{\phi}(y, z|x), p_{\psi}(y, z))) \quad (1)$$

where:

- q_{ϕ} denotes the distribution over the 32×32 encoded tokens generated by dVAE encoder from the image x .

- p_{θ} denotes the distribution over the reconstructed image \hat{x} from dVAE decoder.
- p_{ψ} denotes the joint distribution over the text and image tokens modeled by the transformer.

In Stage 1, dVAE (*or other VQ-VAE variants*) learns to minimize the reconstruction loss between x and \hat{x} . In Stage 2, an auto-regressive transformer optimizes two negative log-likelihood (NLL) losses: (i) for caption y and (ii) for encoded image tokens z .

3.2. Proposed Approach: L-Verse Framework

Inspired by DALL-E [31], we propose two major improvements for high-fidelity image reconstruction and bidirectional image-text generation:

- We improve the diversity of a visual codebook Z with cross-level feature augmentation. We first train multi-level (hierarchical) VQ-VAE (*blue* in Figure 2) and apply weight-sharing to vector quantizers [32, 41] in each feature-level. The hierarchical VQ-VAE is then fine-tuned to a VQ-VAE with codebook size $N = 32 \times 32$.
- We use the segment embedding to indicate whether each token is given as a conditional reference ([REF]) or a generation target ([GEN]). For example, [REF] is added to each text token and [GEN] is added to each image token for text-to-image generation.



Figure 3. Comparison of input images (*top*), reconstructions from multi-level (hierarchical) feature-augmented variational autoencoder (AugVAE-ML) (*middle*), and reconstructions from single-level feature-augmented variational autoencoder (AugVAE-SL) (*bottom*) on Imagenet1K validation set (256 × 256 pixels).

Following subsections describe the training and sampling procedure of L-Verse in detail. The overview of L-Verse framework with actual reconstruction and generation examples are shown in Figure 2.

3.3. Feature-Augmented Variational Autoencoder

Razavi *et al.* [32] states that increasing the number of latent feature map adds extra details to the reconstruction. However, increasing the number of latent map also increases the total codebook size N , from $32 \times 32 = 1024$ [41] to $32 \times 32 + 64 \times 64 = 1152$ [32].

For the high-quality image reconstruction at low-cost, we choose to use the single 32×32 latent map and augment the visual codebook Z instead. From the example in Figure 4, similar patterns in various patch sizes can appear both in one image (*blue*) and across different images (*red*). As the distance between similar patterns gets closer after vector quantization (VQ) [41], extracting patches from different latent maps and storing them in one place removes duplicates and fills the codebook with unique 8192 (d_Z) possible values.

We optimize the encoder - vector quantizer - decoder architecture of VQ-VAE [41] for cross-level feature augmentation:

- We define the encoder as $x' = E(x, f, d_{out})$, where x is an $n \times n \times d_{in}$ tensor and f is a downsampling factor. $E(f, d_{out})$ downsamples x into a $\frac{n}{f} \times \frac{n}{f} \times d_{out}$ tensor x' .

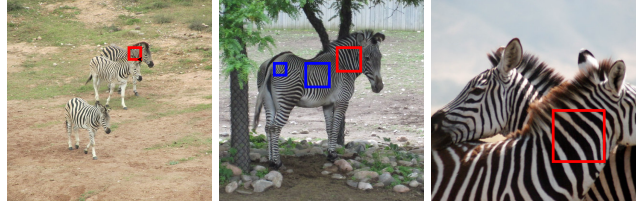


Figure 4. Cross-level patch similarity inside an image (*blue*) and across images (*red*). Our feature-augmented variational autoencoder (AugVAE) utilizes the cross-level patch similarity to diversify the feature codebook.

- We define the vector quantizer as $\hat{z} = VQ(z, d_Z)$, where z is an $n \times n \times d$ tensor with continuous d -size vectors. \hat{z} is a quantized version of z with d_Z possible values for each d -size feature vector. We use exponential-moving-average (EMA) vector quantizer [32]. All vector quantizers in AugVAE share the same weights.
- We define the decoder as $x = G(x', f', d'_{out})$, where \hat{z} is an $n \times n \times d_{in}$ tensor and f' is a upsampling factor. $G(f', d'_{out})$ upsamples $n' \times n' \times d_{in}$ tensor x' into a $n'f' \times n'f' \times d'_{out}$ tensor x .

Hierarchical AugVAE (AugVAE-ML) consists of one $E(4, 256)$ and three $E(2, 256)$, four $VQ(8192)$ with shared weights, and one $G(4, 3)$ and three $G(2, 256)$. As shown in Figure 2 with *blue dotted and connected lines*, $E(x, 4)$ first downsamples a $256 \times 256 \times 3$ RGB image into a $64 \times 64 \times 256$ latent feature tensor. Each $E(2, 256)$ downsamples the previous tensor by 2. In total, four latent feature tensors ($64 \times 64 \times 256$, $32 \times 32 \times 256$, $16 \times 16 \times 256$, and $8 \times 8 \times 256$) are extracted. These four tensors are quantized with a $VQ(8192)$ for each latent map. During the training of AugVAE-ML, each codebook with 8192 values gains diversity via weight sharing. Each $G(2, 256)$ upsamples the concatenation of previous tensor (if exists) and \hat{z} of each level by 2. $G(4, 3)$ reconstructs the original input from the last latent tensor and the quantized vector.

To reduce the overall codebook size N , we finetune the AugVAE-ML into a single-level AugVAE (AugVAE-SL) of 32×32 latent map. We remove encoders and decoders with 16×16 and 8×8 latent map and replace the concatenation before each decoder with a 1×1 convolution to expand the last channel of previous latent tensor by 2. This modification to AugVAE-ML effectively stabilizes the finetuning process. The final architecture of AugVAE is depicted in Figure 2 with *blue connected lines*. As shown in Figure 3, AugVAEs can compress and reconstruct images with high-fidelity. Implementation details of AugVAE architecture and training hyperparameters are provided in Appendix A.

3.4. Bidirectional Auto-Regressive Transformer

With the *masked dot-product multi-head attention*, the conventional auto-regressive transformer [3] can only understand a given sequence from *left to right*. Bidirectional generation between text and image doesn’t require a transformer to be fully-bidirectional: learning how to distinguish an `image \rightarrow text` sequence and a `text \rightarrow image` sequence is enough.

We just tell our bidirectional auto-regressive transformer (BiART) whether the given text (or image) is a *conditional reference* ([REF]) or a *generation target* ([GEN]). We feed BiART with an extra sequence of segment indexes for each token. A learnable embedding vector is assigned to each segment index ([REF]) and ([GEN]) and added to the input sequence. This simple idea enables the training and sampling of bidirectional image-text generation with BiART.

For training, we feed the input sequence in `text \rightarrow image` or `image \rightarrow text` order alternately for each iteration. In each iteration, BiART optimizes two negative log-likelihood (NLL) losses: (i) for the conditional reference y indexed as [REF] and (ii) for the generation target x indexed as [GEN]. When converges, BiART performs text-to-image (*connected red line in Figure 2*) and image-to-text (*dotted red line in Figure 2*) generations without any fine-tuning.

3.5. Training Details

Architecture Overview We first train 100-million parameter AugVAE-SL on ImageNet1K [8]. From results in Figure 3, 5 and Table 1, our AugVAE-SL shows impressive reconstruction results for both in-domain and out-of-domain images. We use ImageNet1K-trained AugVAE-SL as encoder and decoder of L-Verse and pair encoded tokens with corresponding text tokens. BiART in L-Verse is 500-million parameter GPT [3] transformer. While DALL-E [31] and CogView [10] use a sparse-transformer [4] with custom attention masks for fast training and sampling, we use a GPT-style [3] full-transformer to model the bidirectional cross-modal representation between image and text. We use 64 BPE-encoded [36] text tokens with 49808 possibilities and 1024 encoded image tokens with 8192 possibilities. More details are provided in Appendix B.

Mixed Precision Training To save computational cost and sampling time, BiART is trained with FP16 (O2) mixed-precision training without inefficient stabilization methods like PB-relaxation [10] or Sandwich-LayerNorm [10]. These techniques are designed to eliminate the overflow in forward pass, but computationally inefficient. We instead inference the AugVAE in FP32 to prevent the underflow caused by the vector quantizer. Since we freeze

AugVAE for Stage 2, only forward pass is performed.

Ding *et al.* [10] states that the precision problem in language-only training is not so significant as in text-to-image training. They hypothesize the heterogeneity of data as the cause. We found that training a transformer in bidirectional manner relieves the heterogeneity between image and text, and leads to a stable training. In our toy experiments, BiART converged faster and showed better performance compared to text-to-image or image-to-text unidirectional auto-regressive transformers. This states that bidirectional training approach with segment embedding is not only useful in the application-level, but also can be a new fundamental to find the cross-modal representation between different data domains.

3.6. Sampling Details

Image Sampling Similar to Ramesh *et al.* [31], we rerank samples drawn from BiART using a pretrained contrastive model, CLIP [30]. CLIP assigns a score (*clip-score*) based on how well the image and text match with each other. For text-to-image generation, we make 64 samples from trained L-Verse model and calculate the *clip-score* to select a Top 1 image. We repeat this process k times with different random seeds to sample k images in total.

Text Sampling Our L-Verse auto-regressively generates a sequence of tokens. To generate an RGB image, 1024 (32×32) tokens should be generated one-by-one. However, the length of text may vary depending on its reference image. For this reason, generating full 64 tokens doesn’t always guarantee the quality of sampled text. In worst case, the result caption can be just a repeated sequence of same sentence and [PAD] tokens. From the statistics of MS-COCO Captions [24], each caption contains average 16 words. We first sample 32 text tokens for each reference image and split the result caption by the full stop (.) token. We only use the first split to calculate the *clip-score* for reranking. This process dramatically saves computation time to generate 64 samples and select Top 1.

From machine evaluation metrics in Table 2, truncated captions from 32 tokens achieve new state-of-the-art in all metrics except CIDEr [43] among the peers trained only on MS-COCO Captions. L-Verse also shows comparable performance to OSCAR [23], which is pretrained on 6.5-million image-text pairs. While full 64 token captions score 181.6 in CIDEr and 28.9 in SPICE [1], we figured out that scores are high just because each caption has more meaningful words. In our inner-group examination between full and truncated captions, we have agreed that each truncated version is more concise and accurate. We further investigate the quality of L-Verse generated captions with human evaluation, in comparison with human labeled ground-truths.

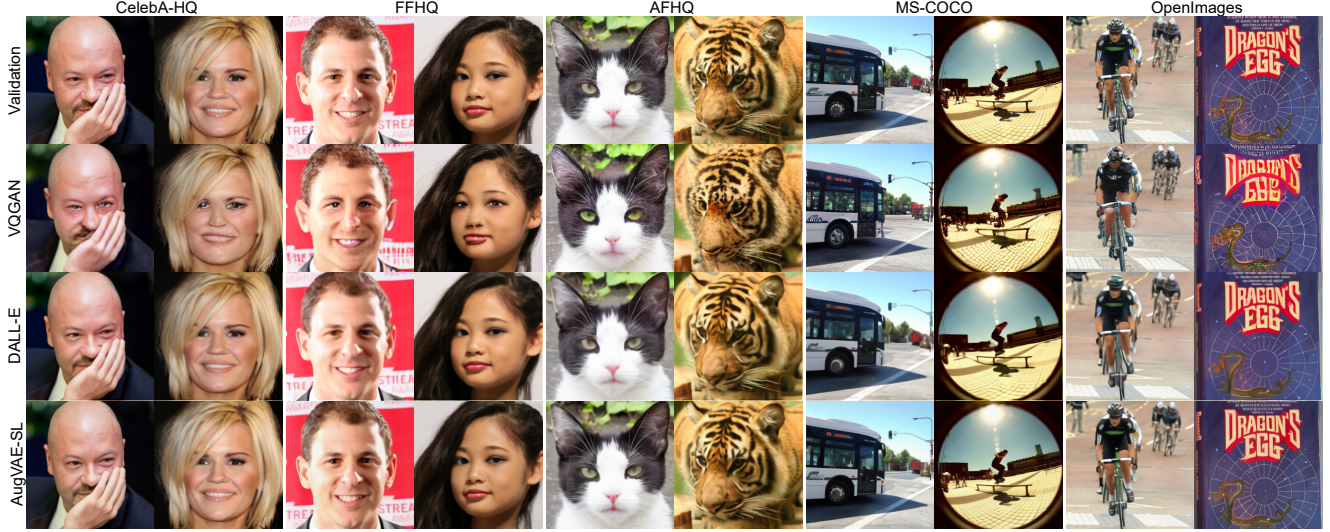


Figure 5. Qualitative evaluation on the reconstruction performance of different VQVAEs with unseen image domains. For all settings, we use ImageNet1K trained models without any finetuning. Images are resized to 256×256 by a LANCZOS [6] filter. Cross-level feature augmentation allows AugVAE-SL to express out-of-domain unseen images in high-fidelity. Please zoom in for the detailed comparison.

Model	Codebook Size N	d_Z	FID
DALL-E [31]	32×32	8192	32.01
VQGAN [12]	16×16	1024	7.94
VQGAN [12]	16×16	16384	4.98
AugVAE-SL	32×32	8192	3.28
VQVAE-2 [32]	$64 \times 64 \& 32 \times 32$	512	~ 10
VQGAN [12]	$64 \times 64 \& 32 \times 32$	512	1.45
AugVAE-ML	$64 \times 64 \sim 8 \times 8$	8192	1.04

Table 1. Reconstruction Fréchet Inception Distance (FID) on ImageNet1K validation set. d_Z : The number of unique feature vectors in codebook. Both multi-level (hierarchical) feature-augmented variational autoencoder (AugVAE-ML) and single-level feature-augmented variational autoencoder (AugVAE-SL) achieve lowest FID among their peers.

4. Experiments

In this section, we demonstrate the performance of proposed L-Verse in every aspects with both quantitative and qualitative experiments. We mainly discuss reconstruction performance on ImageNet1K [8] and out-of-domain unseen images, image-to-text generation (image captioning) results on MS-COCO Captions [24], text-to-image generation results on MS-COCO Captions. For MS-COCO, we trained L-Verse on MS-COCO Captions 2014 *Karpathy* splits for fair evaluation with previous methods. We also include results of L-Verse trained on Conceptual Captions [37] to further discuss the scalability of L-Verse architecture for

zero-shot text-to-image generation. The FID can change depending on calculation tools. For fair comparison, we compute the Reconstruction FID with `torch-fidelity` [29], caption evaluation metrics in Table 2 with `nlg-eval` [38], and FIDs in Table 3 with the DM-GAN code [50], available at <https://github.com/MinfengZhu/DM-GAN>.

4.1. Image Reconstruction

As Esser *et al.* [12] stated, the reconstruction Fréchet Inception Distance (FID) [16] of a VQ-VAE provide a lower bound on the achievable FID of the generative model trained on it. From the results on ImageNet1K validation set in Table 1, our AugVAE-ML trained with novel *cross-level feature augmentation* achieves FID of **1.04**, meaning AugVAE-ML can compress and reconstruct image without nearly any information loss. Reconstruction examples on Figure 3 also demonstrates AugVAE-ML’s qualitative performance. Finetuned from AugVAE-ML, our AugVAE-SL also achieves new state-of-the-art FID of **3.28** among its single-level peers. In a more difficult setting, we evaluate AugVAE-SL on reconstructing *out-of-domain* unseen images. From the examples in Figure 5, AugVAE-SL trained on ImageNet1K shows impressive reconstruction fidelity for all validation input images without extra finetuning. From this result, we believe that our AugVAE-SL can work as a new “*imagenet-backbone*” for various vision tasks. Detailed examination with more examples for each dataset in Figure 5 can be found in Appendix C.

Model	B-4	M	R	C	S
SCST [34]	34.2	26.7	55.7	114.0	-
Up-Down [2]	36.3	27.7	56.9	120.1	21.4
RFNet [39]	36.5	27.7	57.3	121.9	21.2
Up-Down+HIP [47]	38.2	28.4	58.3	127.2	21.9
GCN-LSTM [28]	38.2	28.5	58.3	127.6	22.0
SGAE [46]	38.4	28.4	58.6	127.8	22.1
ORT [15]	38.6	28.7	58.4	128.3	22.6
AOANet [17]	38.9	29.2	58.8	129.8	22.4
M^2 Transformer [7]	39.1	29.2	58.6	131.2	22.6
L-verse	39.9	31.4	60.4	102.2	23.3
*L-verse	27.6	23.6	43.9	181.6	28.9
[†] OSCAR _B [23]	40.5	29.7	-	137.6	22.8
[†] OSCAR _L [23]	41.7	30.6	-	140.0	24.5

⁻ **B-4**: BLEU-4 **M**: METEOR **R**: ROUGE **C**: CIDEr **S**: SPICE

* Captions generated without truncation.

[†] Models pretrained on 6.5 million image-text pairs.

Table 2. Comparison with state-of-the-arts on MS-COCO Captions *Karpathy* test split. We mainly compare results with models trained only on MS-COCO. Results from OSCAR (which requires additional fine-tuning) is given as a reference.

4.2. Image-to-Text Generation

We evaluate the image-to-text generation (image captioning) performance of L-Verse with (*i*) machine evaluation metrics against previous MS-COCO trained state-of-the-arts and (*ii*) human evaluation against corresponding ground-truth captions.

Machine Evaluation We first compare the performance of our model with MS-COCO trained image captioning models in Table 2. We also include OSCAR [23], which is finetuned from a pretrained model with 6.5-million image-text pairs, to assess the scalability of our model with larger dataset. With proposed sampling method in Section 3.6, L-Verse surpasses all the other methods in terms of BLEU-4, METEOR, ROUGE, and SPICE without any object detection framework or other extra information. L-Verse also shows comparable performance to OSCAR, showing that pretraining L-Verse on a larger set of image-text pairs is a promising direction for future work.

Human Evaluation Without caption truncation, L-Verse achieves the highest score in CIDEr and SPICE. As we stated in Section 3.6, machine evaluation metrics don’t always guarantee the qualitative performance of generated captions. We further conduct a human evaluation similar to the one used in Li *et al.* [22]. We directly evaluate L-Verse generated captions with human-labeled ground-truth captions, which is the theoretical upper-bound of L-Verse



Figure 6. Examples of captions generated by L-Verse with corresponding ground-truths. Examples are sampled from conducted human evaluation results which received “*Both captions well describe the image*”.

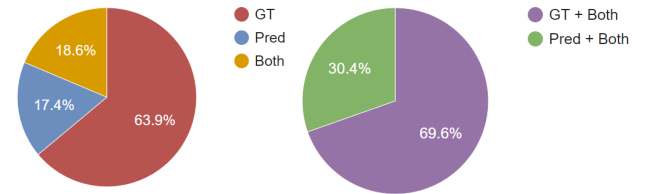


Figure 7. Human evaluation results on MS-COCO Captions *mini-val* split. With question “*Which caption well describes the given image?*”, L-Verse generated captions received **30.4%** of votes (Pred + Both) in total.

in image-to-text generation. We randomly sample 500 sets of images, corresponding ground-truth caption (GT), and L-Verse generated caption (Pred) from MS-COCO 2014 *mini-val* split for the evaluation pool. 150 anonymous people participated for the evaluation. For each participant, we show randomly sampled 50 sets of image, GT, and Pred from the pool and ask to choose the best caption for each set. To cope with **tie** situation, we also allow each participant to choose “*Both captions well describe the image*”. We provide more details on human evaluation in Appendix D. Results in Figure 7 show that L-Verse can generate a detailed explanation of a given image, receiving **30.4%** of votes (Pred + Both) in total. Examples in Figure 6 also demonstrate that L-Verse doesn’t miss the detail of each image.

Model	FID-0	FID-1	FID-2	FID-4	FID-8
AttnGAN [45]	35.2	44.0	72.0	108.0	100.0
DM-GAN [50]	26.0	39.0	73.0	119.0	112.3
DF-GAN [40]	26.0	33.8	55.9	91.0	97.0
L-Verse	45.8	41.9	35.5	30.2	29.83
*L-Verse-CC	37.2	31.6	25.7	21.4	21.1
†DALL-E [31]	27.5	28.0	45.5	83.5	85.0
†CogView [10]	27.1	19.4	13.9	19.4	23.6

^{*} **FID- k :** FID of images blurred by radius k Gaussian filter.

^{*} L-Verse trained on Conceptual Captions.

[†] Models trained on over 30 million image-text pairs.

Table 3. Fréchet Inception Distance (FID) on a subset of 30,000 captions sampled from MS-COCO Captions validation set. We mainly compare results with models trained only on MS-COCO. In the bottom part of the table, we provide results from DALL-E, CogView, and L-Verse-CC (which are trained from much larger datasets) as references.

4.3. Text-to-Image Generation

Following Ramesh *et al.* [31] and Ding *et al.* [10], we evaluate the text-to-image generation performance of L-Verse by comparing it to prior approaches. We compute FIDs in Table 3 after applying a Gaussian filter with varying radius to both validation images and samples from L-Verse. We use the image sampling process explained in Section 3.6. Generated samples with corresponding captions from MS-COCO are provided in Appendix E.

According to Ramesh *et al.* [31], training a transformer on tokens from a VQ-VAE encoder disadvantages model since it generates a image in low-frequency domain. Trained on same MS-COCO training set, L-Verse achieves best FID among previous approaches by a large margin with a slight blur of radius 2. The gap tends to increase as the blur radius is increased. We also compare L-Verse-CC, L-Verse trained on Conceptual Captions [37], with DALL-E [31] and CogView [10]. Considering the size of training data, L-Verse shows comparable text-to-image generation performance to other large-scale transformers as blur radius increases.

It is interesting that L-Verse shows decreasing FID with increasing blur radius, while other models show increasing FID. We hypothesize that L-Verse focuses on objects in the reference text, showing lower FIDs when high-frequency details are lost. This finding also corresponds with image-to-text generation results in Section 4.2. We also provide initial zero-shot text-to-image generation results with L-Verse in Figure 8. Trained on Conceptual Captions [37], L-Verse generates detailed images with objects in reference texts. We believe that L-Verse will also be able to generate realistic images in zero-shot fashion when trained with sufficient data and scale.

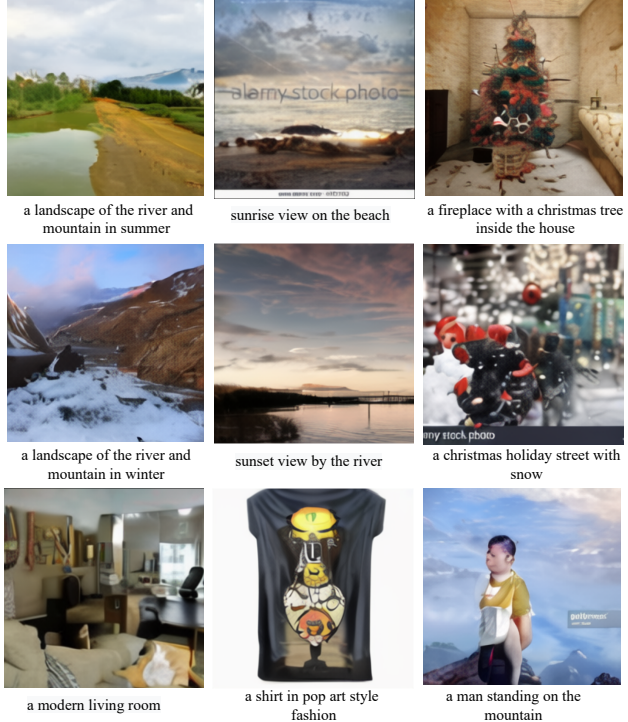


Figure 8. Examples of zero-shot text-to-image generation. Results are sampled from L-Verse-CC, which is trained on 3-million image-text pairs from Conceptual Captions.

4.4. Effects of Bidirectional Learning

L-Verse internally learns a *reversible and densely connected* mapping between images and texts. From this, L-Verse can generate a text or an image in accordance with the given condition without any finetuning or extra object detection frameworks. Bidirectional learning not only saves the time and computational cost for training and application. As we mentioned in Section 3.5, our bidirectional approach also mitigates the heterogeneity of data and enables stable FP16 (O2) mixed-precision training.

5. Conclusion

This paper presents L-Verse, a novel framework for bidirectional generation between image and text. Our *feature-augmented variational autoencoder* (AugVAE) achieves new state-of-the-art reconstruction FID and shows its potential as an universal backbone encoder-decoder for generative models. We also enable bidirectional training of auto-regressive transformer with the *segment embedding*. Proposed *bidirectional auto-regressive transformer* (BiART) learns both text-to-image and image-to-text as a whole. Experimental results demonstrate that our L-Verse framework shows remarkable performances in both image-to-text and text-to-image generation tasks.

References

[1] Peter Anderson, Basura Fernando, Mark Johnson, and Stephen Gould. Spice: Semantic propositional image caption evaluation, 2016. 5

[2] Peter Anderson, Xiaodong He, Chris Buehler, Damien Teney, Mark Johnson, Stephen Gould, and Lei Zhang. Bottom-up and top-down attention for image captioning and visual question answering, 2018. 7

[3] T. Brown, B. Mann, Nick Ryder, Melanie Subbiah, J. Kaplan, P. Dhariwal, Arvind Neelakantan, Pranav Shyam, Girish Sastry, Amanda Askell, Sandhini Agarwal, Ariel Herbert-Voss, G. Krüger, Tom Henighan, R. Child, Aditya Ramesh, D. Ziegler, Jeffrey Wu, Clemens Winter, Christopher Hesse, Mark Chen, E. Sigler, Mateusz Litwin, Scott Gray, Benjamin Chess, J. Clark, Christopher Berner, Sam McCandlish, A. Radford, Ilya Sutskever, and Dario Amodei. Language models are few-shot learners. *ArXiv*, abs/2005.14165, 2020. 1, 2, 3, 5, 11

[4] Rewon Child, Scott Gray, Alec Radford, and Ilya Sutskever. Generating long sequences with sparse transformers, 2019. 1, 2, 5

[5] Yunjey Choi, Youngjung Uh, Jaejun Yoo, and Jung-Woo Ha. Stargan v2: Diverse image synthesis for multiple domains. In *Proceedings of the IEEE Conference on Computer Vision and Pattern Recognition*, 2020. 11

[6] M. A. Clark, Chulwoo Jung, and Christoph Lehner. Multi-grid lanczos. *EPJ Web of Conferences*, 175:14023, 2018. 6, 11

[7] Marcella Cornia, Matteo Stefanini, Lorenzo Baraldi, and Rita Cucchiara. Meshed-memory transformer for image captioning. In *Proceedings of the IEEE/CVF Conference on Computer Vision and Pattern Recognition (CVPR)*, June 2020. 1, 2, 7

[8] J. Deng, W. Dong, R. Socher, L.-J. Li, K. Li, and L. Fei-Fei. ImageNet: A Large-Scale Hierarchical Image Database. In *CVPR*, 2009. 2, 5, 6, 11

[9] Jacob Devlin, Ming-Wei Chang, Kenton Lee, and Kristina Toutanova. Bert: Pre-training of deep bidirectional transformers for language understanding, 2019. 1, 2

[10] Ming Ding, Zhuoyi Yang, Wenyi Hong, Wendi Zheng, Chang Zhou, Da Yin, Junyang Lin, Xu Zou, Zhou Shao, Hongxia Yang, and Jie Tang. Cogview: Mastering text-to-image generation via transformers. *arXiv preprint arXiv:2105.13290*, 2021. 1, 2, 5, 8

[11] Patrick Esser, Robin Rombach, Andreas Blattmann, and Björn Ommer. Imagebart: Bidirectional context with multinomial diffusion for autoregressive image synthesis, 2021. 1

[12] Patrick Esser, Robin Rombach, and Björn Ommer. Taming transformers for high-resolution image synthesis. In *Proceedings of the IEEE/CVF Conference on Computer Vision and Pattern Recognition (CVPR)*, pages 12873–12883, June 2021. 1, 2, 6, 11

[13] Ian Goodfellow, Jean Pouget-Abadie, Mehdi Mirza, Bing Xu, David Warde-Farley, Sherjil Ozair, Aaron Courville, and Yoshua Bengio. Generative adversarial nets. In Z. Ghahramani, M. Welling, C. Cortes, N. D. Lawrence, and K. Q. Weinberger, editors, *Advances in Neural Information Processing Systems 27*, pages 2672–2680. Curran Associates, Inc., 2014. 2

[14] Kaiming He, Xiangyu Zhang, Shaoqing Ren, and Jian Sun. Deep residual learning for image recognition. In *Proceedings of the IEEE conference on computer vision and pattern recognition*, pages 770–778, 2016. 11

[15] Simao Herdade, Armin Kappeler, Kofi Boakye, and Joao Soares. Image captioning: Transforming objects into words, 2020. 7

[16] Martin Heusel, Hubert Ramsauer, Thomas Unterthiner, Bernhard Nessler, and Sepp Hochreiter. Gans trained by a two time-scale update rule converge to a local nash equilibrium. In *NIPS*, 2017. 6

[17] Lun Huang, Wenmin Wang, Jie Chen, and Xiao-Yong Wei. Attention on attention for image captioning, 2019. 7

[18] Eric Jang, Shixiang Gu, and Ben Poole. Categorical reparameterization with gumbel-softmax, 2017. 2

[19] Tero Karras, Samuli Laine, and Timo Aila. A style-based generator architecture for generative adversarial networks, 2019. 11

[20] Diederik P Kingma and Max Welling. Auto-encoding variational bayes, 2014. 3

[21] Alina Kuznetsova, Hassan Rom, Neil Alldrin, Jasper Uijlings, Ivan Krasin, Jordi Pont-Tuset, Shahab Kamali, Stefan Popov, Matteo Malloci, Alexander Kolesnikov, and et al. The open images dataset v4. *International Journal of Computer Vision*, 128(7):1956–1981, Mar 2020. 11

[22] Jiwei Li, Will Monroe, Alan Ritter, Michel Galley, Jianfeng Gao, and Dan Jurafsky. Deep reinforcement learning for dialogue generation, 2016. 7

[23] Xiujun Li, Xi Yin, Chunyuan Li, Pengchuan Zhang, Xiaowei Hu, Lei Zhang, Lijuan Wang, Houdong Hu, Li Dong, Furu Wei, Yejin Choi, and Jianfeng Gao. Oscar: Object-semantics aligned pre-training for vision-language tasks, 2020. 5, 7

[24] Tsung-Yi Lin, Michael Maire, Serge Belongie, Lubomir Bourdev, Ross Girshick, James Hays, Pietro Perona, Deva Ramanan, C. Lawrence Zitnick, and Piotr Dollár. Microsoft coco: Common objects in context, 2015. 2, 5, 6, 11

[25] Ziwei Liu, Ping Luo, Xiaogang Wang, and Xiaoou Tang. Deep learning face attributes in the wild. In *Proceedings of International Conference on Computer Vision (ICCV)*, 2015. 11

[26] Ilya Loshchilov and Frank Hutter. Fixing weight decay regularization in adam. *CoRR*, abs/1711.05101, 2017. 11

[27] Chris J. Maddison, Andriy Mnih, and Yee Whye Teh. The concrete distribution: A continuous relaxation of discrete random variables, 2017. 2

[28] Diego Marcheggiani and Ivan Titov. Encoding sentences with graph convolutional networks for semantic role labeling, 2017. 7

[29] Anton Obukhov, Maximilian Seitzer, Po-Wei Wu, Semen Zhydenko, Jonathan Kyl, and Elvis Yu-Jing Lin. High-fidelity performance metrics for generative models in pytorch, 2020. Version: 0.3.0, DOI: 10.5281/zenodo.4957738. 6

[30] Alec Radford, Jong Wook Kim, Chris Hallacy, Aditya Ramesh, Gabriel Goh, Sandhini Agarwal, Girish Sastry, Amanda Askell, Pamela Mishkin, Jack Clark, Gretchen Krueger, and Ilya Sutskever. Learning transferable visual models from natural language supervision, 2021. 5

[31] Aditya Ramesh, Mikhail Pavlov, Gabriel Goh, Scott Gray, Chelsea Voss, Alec Radford, Mark Chen, and Ilya Sutskever. Zero-shot text-to-image generation, 2021. 1, 2, 3, 5, 6, 8

[32] Ali Razavi, Aaron van den Oord, and Oriol Vinyals. Generating diverse high-fidelity images with vq-vae-2, 2019. 1, 2, 3, 4, 6

[33] Shaoqing Ren, Kaiming He, Ross Girshick, and Jian Sun. Faster r-cnn: Towards real-time object detection with region proposal networks. In *Advances in neural information processing systems*, pages 91–99, 2015. 2

[34] Steven J. Rennie, Etienne Marcheret, Youssef Mroueh, Jarret Ross, and Vaibhava Goel. Self-critical sequence training for image captioning, 2017. 7

[35] Danilo Jimenez Rezende, Shakir Mohamed, and Daan Wierstra. Stochastic backpropagation and approximate inference in deep generative models. *arXiv preprint arXiv:1401.4082*, 2014. 3

[36] Rico Sennrich, Barry Haddow, and Alexandra Birch. Neural machine translation of rare words with subword units, 2016. 5

[37] Piyush Sharma, Nan Ding, Sebastian Goodman, and Radu Soricut. Conceptual captions: A cleaned, hypernymed, image alt-text dataset for automatic image captioning. In *Proceedings of ACL*, 2018. 2, 6, 8, 11

[38] Shikhar Sharma, Layla El Asri, Hannes Schulz, and Jeremie Zumer. Relevance of unsupervised metrics in task-oriented dialogue for evaluating natural language generation. *CoRR*, abs/1706.09799, 2017. 6

[39] Xuelun Shen, Cheng Wang, Xin Li, Zenglei Yu, Jonathan Li, Chenglu Wen, Ming Cheng, and Zijian He. Rf-net: An end-to-end image matching network based on receptive field, 2019. 7

[40] Ming Tao, Hao Tang, Songsong Wu, Nicu Sebe, Xiao-Yuan Jing, Fei Wu, and Bingkun Bao. Df-gan: Deep fusion generative adversarial networks for text-to-image synthesis, 2021. 2, 8

[41] Aaron van den Oord, Oriol Vinyals, and Koray Kavukcuoglu. Neural discrete representation learning, 2018. 1, 2, 3, 4

[42] Ashish Vaswani, Noam Shazeer, Niki Parmar, Jakob Uszkoreit, Llion Jones, Aidan N. Gomez, Łukasz Kaiser, and Illia Polosukhin. Attention is all you need. *ArXiv*, abs/1706.03762, 2017. 1, 2

[43] Ramakrishna Vedantam, C. Lawrence Zitnick, and Devi Parikh. Cider: Consensus-based image description evaluation, 2015. 5

[44] P. Welinder, S. Branson, T. Mita, C. Wah, F. Schroff, S. Belongie, and P. Perona. Caltech-UCSD Birds 200. Technical Report CNS-TR-2010-001, California Institute of Technology, 2010. 2

[45] Tao Xu, Pengchuan Zhang, Qiuyuan Huang, Han Zhang, Zhe Gan, Xiaolei Huang, and Xiaodong He. AttnGAN: Fine-grained text to image generation with attentional generative adversarial networks, 2017. 2, 8

[46] Xu Yang, Kaihua Tang, Hanwang Zhang, and Jianfei Cai. Auto-encoding scene graphs for image captioning, 2018. 7

[47] Ting Yao, Yingwei Pan, Yehao Li, and Tao Mei. Hierarchy parsing for image captioning, 2019. 7

[48] Han Zhang, Jing Yu Koh, Jason Baldridge, Honglak Lee, and Yinfei Yang. Cross-modal contrastive learning for text-to-image generation, 2021. 2

[49] Richard Zhang, Phillip Isola, Alexei A. Efros, Eli Shechtman, and Oliver Wang. The unreasonable effectiveness of deep features as a perceptual metric, 2018. 11

[50] Minfeng Zhu, Pingbo Pan, Wei Chen, and Yi Yang. Dm-gan: Dynamic memory generative adversarial networks for text-to-image synthesis, 2019. 2, 6, 8

A. Details for AugVAE

A.1. Architecture

The AugVAE encoder and decoder are ResNet [14] with bottleneck-style resblocks. Our AugVAE is specifically based on the encoder-decoder from official VQGAN [12] implementation available at <https://github.com/CompVis/taming-transformers>. From VQGAN Implementation, we removed the attention block and applied the modification we describe in 3.3. The high-level architecture of our AugVAE is depicted in Figure 9.

A.2. Training

Our AugVAE is trained on ImageNet1K [8]. We resize each image into $256 \times 256 \times 3$ and apply random crop with 0.75 crop ratio. We only apply random crop for training. We train both AugVAE-ML and AugVAE-SL using AdamW [26] optimizer with $\beta_1 = 0.9$, $\beta_2 = 0.999$, $\epsilon = 10e-8$, weight decay multiplier $1e-5$, and the learning rate $4.5e-6$ multiplied by the batch size. We half the learning rate each time the training loss appeared to plateau. For the loss term, we use a combination of mean-squared-error (MSE) and LPIPS [49] losses between the input and the reconstructed image. For stable training, we multiply the LPIPS loss by 0.1.

B. Details for BiART

B.1. Architecture

Our BiART is similar to the GPT architecture [3]. We utilize the minGPT implementation of GPT architectures available at <https://github.com/karpathy/minGPT>. We only add the segment embedding with dimension size 256 for [REF] and [GEN]. Each segment embedding is added to the positional encoding of an input token. We use a 32-layer decoder-only transformer with 1024 dimensional states and 16 masked self-attention heads.

B.2. Training

The BiART is trained on MS-COCO Captions [24] and Conceptual Captions [37]. We first resize each image into $256 \times 256 \times 3$ and apply random crop with 0.75 crop ratio. We only apply random crop for training. We also apply 10% BPE Dropout when BPE-encoding the captions for training. We train BiART using AdamW [26] optimizer with $\beta_1 = 0.9$, $\beta_2 = 0.95$, $\epsilon = 1e-8$, weight decay multiplier $1e-2$, and the learning rate $4.5e-7$ multiplied by the batch size. We don't apply the weight decay to the embedding parameters. We half the learning rate each time the training loss appeared to plateau.

Dataset	FID
CelebA-HQ [25]	7.24
FFHQ [19]	4.92
AFHQ [5]	4.36
MS-COCO [24]	4.77
OpenImages V6 [21]	3.15

Table 4. Reconstruction Fréchet Inception Distance (FID) of AugVAE on various datasets. For all settings, we use ImageNet1K trained AugVAE-SL without any finetuning on each dataset. Images are resized to 256×256 with LANCZOS [6] filter.

C. Examples for Image Reconstruction

We provide more examples of in-domain image reconstruction in Figure 11 and out-of domain in Figure 12. We also provide the reconstruction FID of AugVAE-SL on various datasets in Table 4 as a reference for future works. AugVAE-SL trained on ImageNet1K shows “ ≤ 8 ” FID for all data domain without extra finetuning.

D. Examples for Image-to-Text Generation

We provide an example task interface of our human evaluation we mentioned in Section 4.2 in Figure 10. We also provide more examples of image-to-text generation on MS-COCO Captions in Figure 13. All examples in Figure 13 received “*Both captions well describe the image*” in our human evaluation.

E. Examples for Text-to-Image Generation

We provide examples of text-to-image generation with L-Verse on captions from MS-COCO in Figure 14.

F. Discussion on Potential Negative Impact

Our findings show excellent performances on both image-to-text and text-to-image generation tasks. L-Verse has a wide range of beneficial applications for society, including image captioning, visual question answering, and text visualization. But there are still potential malicious or unintended uses of L-Verse. For this reason, we first provide an open access only to AugVAE for now. To prevent potential negative impact to our society, we will perform additional security risk assessment before we release the full L-Verse framework to the public.

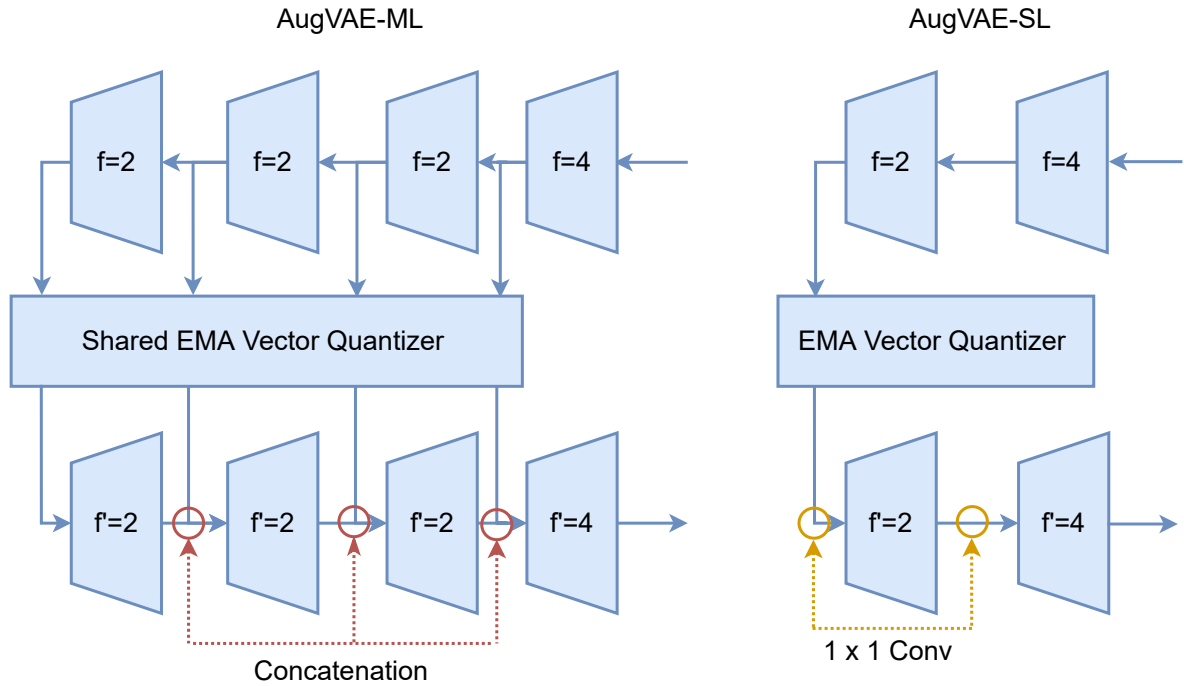


Figure 9. Proposed AugVAE. Trained with cross-level feature augmentation, AugVAE-ML is finetuned into AugVAE-SL to reduce the length of encoded image sequence. We remove unnecessary encoders and decoders from AugVAE-ML and replace the concatenation operation with a 1×1 convolution which expands the last dimension of the input tensor by two.

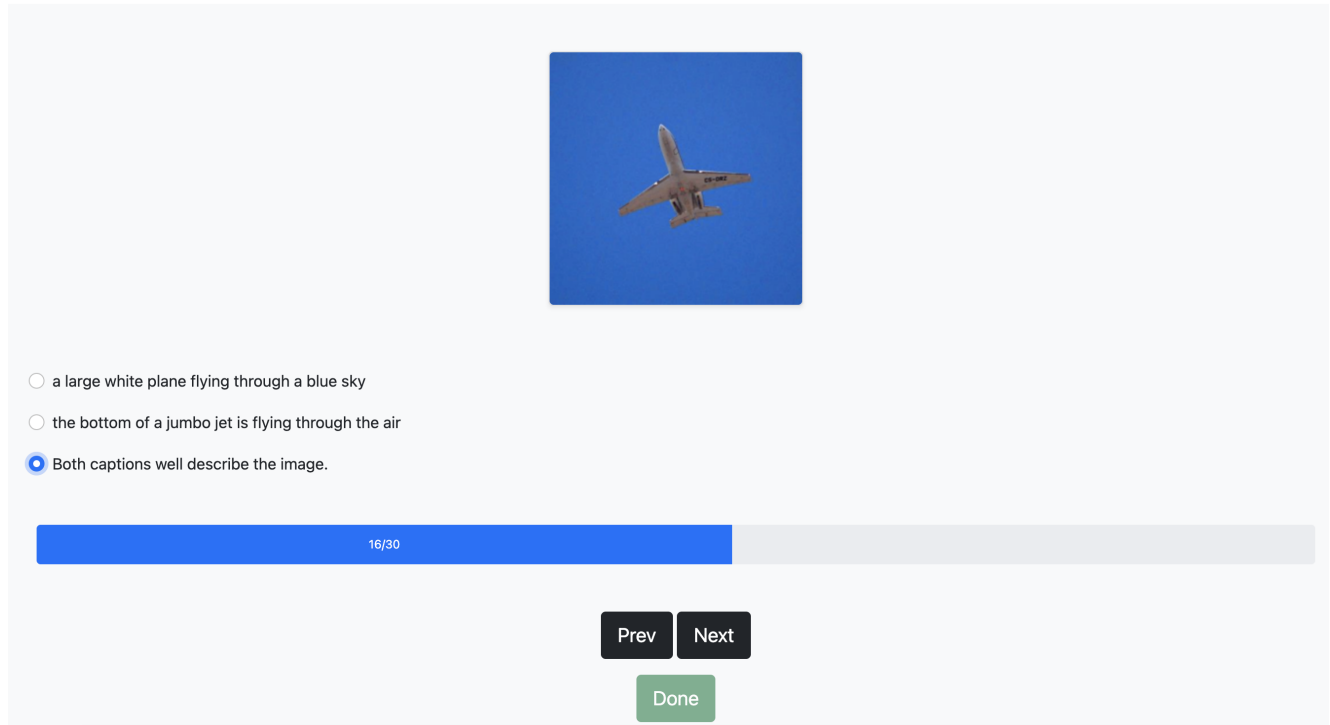


Figure 10. Example interface for human evaluation. Random sampled 30 examples are shown to each participant.

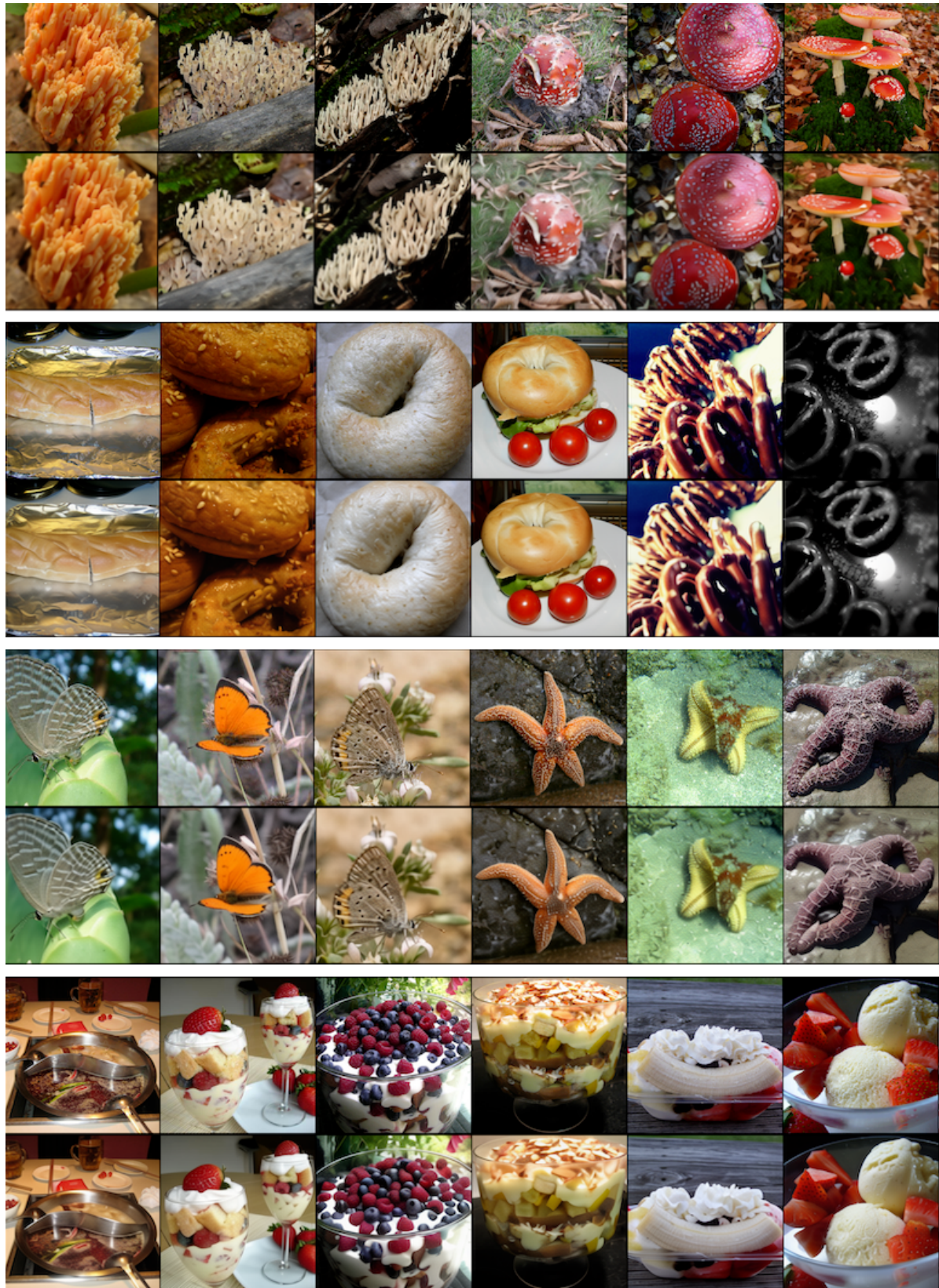


Figure 11. More examples of input images (*top*) and reconstructions from AugVAE-SL (*bottom*) on Imagenet1K validation set (256 × 256 pixels).



Figure 12. More examples of input images (*top*) and reconstructions from AugVAE-SL (*bottom*) with unseen image domains (256 × 256 pixels).

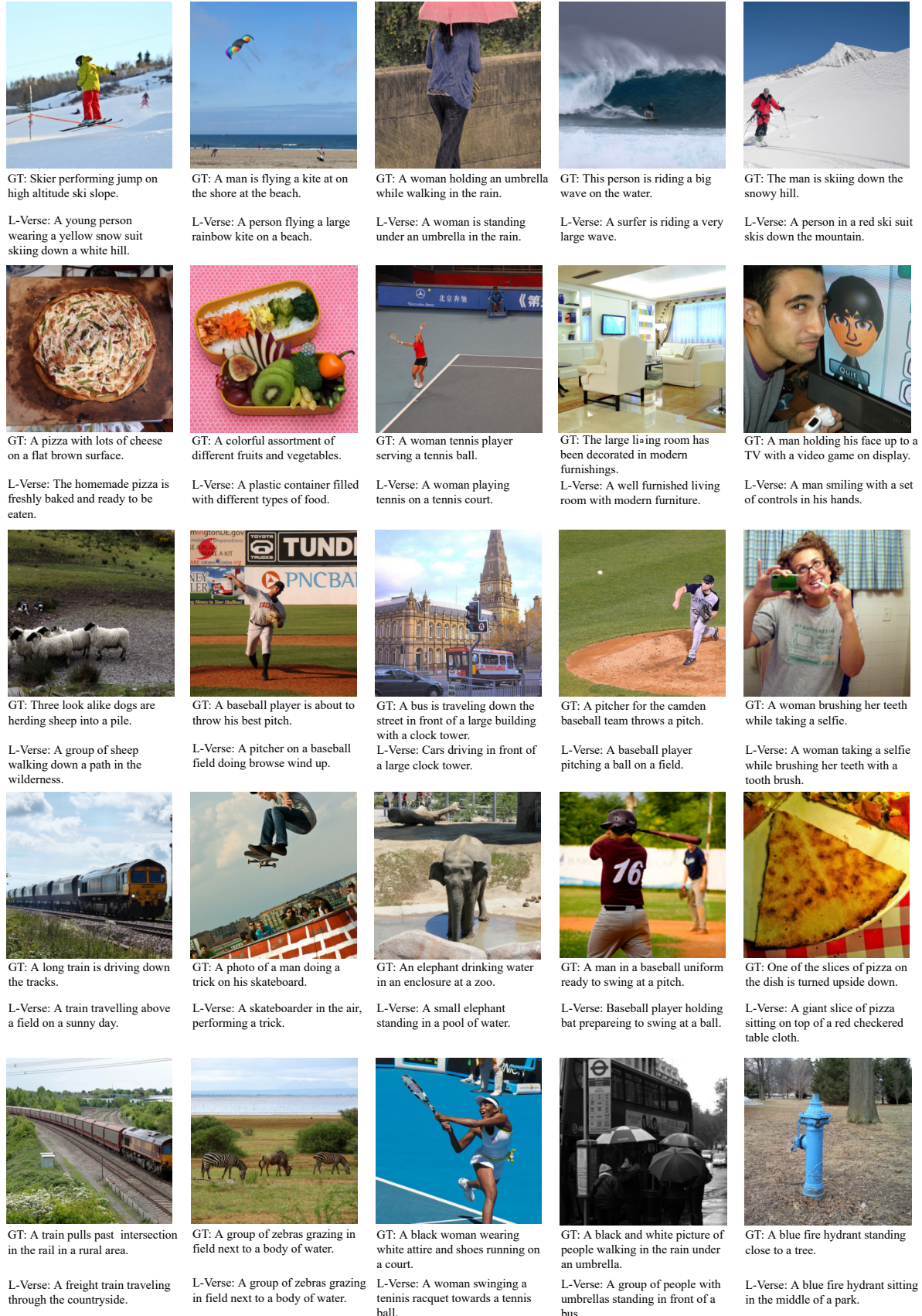


Figure 13. More examples of image-to-text generation on MS-COCO with corresponding ground-truths.



Figure 14. Examples of text-to-image generation on MS-COCO.